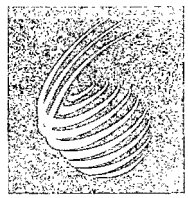

Technical Report
RAL-TR-95-001

Gain and Noise Measurements on Two Avalanche Photodiodes Proposed for the CMS ECAL

J E Bateman S R Burge and R Stephenson

April 1995

COUNCIL FOR THE CENTRAL LABORATORY OF THE RESEARCH COUNCILS

The Central Laboratory for the Research Councils
Library and Information Services
Rutherford Appleton Laboratory
Chilton
Didcot
Oxfordshire
OX11 0QX
Tel: 01235 445384 Fax: 01235 446403
E-mail library@rl.ac.uk

ISSN 1358-6254

GAIN AND NOISE MEASUREMENTS ON TWO AVALANCHE PHOTODIODES PROPOSED FOR THE CMS ECAL

J E Bateman, S R Burge and R Stephenson,
Rutherford Appleton Laboratory, Chilton, Didcot, OX11 0QX,UK

We report comparative laboratory tests on the noise performance of the two avalanche photodiodes used in the 1994 CMS ECAL beam test.

1. INTRODUCTION

It is currently proposed that the electromagnetic calorimeter (ECAL) of CMS be constructed from lead tungstate crystals viewed (at least in the barrel region) by avalanche photodiode (APD) light sensors which would have the advantage of being able to operate in the ambient 4T magnetic field. In summer 1994 a prototype shower detector consisting of 36 crystals viewed by APDs supplied by EG&G and Hamamatsu and serviced by front-end preamplifiers supplied by RAL was tested in a high energy electron beam at CERN. Following these tests [1] (which produced encouraging results) we have studied examples of the two types of device in some detail in the laboratory to try to provide the gain and noise data necessary to predict the performance achievable in the proposed ECAL detector. The EG&G device (for which we have not so far discovered a part number) was kindly loaned to us by Roger Rusack of the University of Minesota and the Hamamatsu device is one of the devices calibrated at RAL for the 1994 beam test. This is a special, low-capacitance version of the Hamamatsu production device type S5345 which we shall refer to as an S5345LC. Both devices have a similar active area ($\approx 20\text{mm}^2$) and (we assume) a similar quantum efficiency and gain range so our questions centred on the noise properties of the APDs.

1.1 APD Structure

All APDs basically possess the structure shown schematically in figure 1; however variations in the materials and processes chosen can sustantially affect the noise properties of the device. As a photon enters the APD it must penetrate the heavily doped contact layer before ionising an atom in the lightly doped conversion region. An electric field of around 10kV/cm pulls the electron into the highly doped junction region where an electric field of greater than 100kV/cm induces carrier multiplication and so amplifies the original signal. A buffer region of low resistivity material permits a thick depletion region to isolate the high-capacitance avalanche junction from the outside world and keep the parasitic capacitance of the device low. A final back-contact electrode completes the circuit. We do not have formal specifications for the thickness of the various regions; informally we understand the following approximate figures. The EG&G diode is understood to have a front contact 0.2μm thick, a conversion region 6μm thick an avalanche region 6μm thick and a drift region 100μm thick. The device is fabricated in high-resitivity single crystal silicon using ion -implantation. About the S5345LC we know little except that the conversion region is believed to be about 12μm thick and that the device is fabricated by epitaxial growth methods.

The relevance of these structural details to our application may be briefly summarised as follows.

Front contact: A thick front contact reduces the sheet resistance and so the effective series noise resistor. If this rises to much more than a few tens of ohms it will contribute significantly to the system white noise. On the other hand at shorter wavelengths (< 500nm) the window electrode can cause significant absorption and so reduce sensitivity.

Conversion Region: At a wavelength of 500nm (the approximate peak of lead tungstate emission) the attenuation length of light in silicon is $\approx 1\mu$m. The 6μm thickness in the EG&G APD is thus adequate for a high quantum efficiency without inducing unnecessary signal from

minimum ionising particles which penetrate the diode (the "nuclear diode" effect). It will be recalled that such a particle deposits ≈ 100 electrons/μm on traversing the APD. Ideally this region should be restricted to a few microns in depth. Another reason for restricting the depth of this region is the thermal generation of bulk leakage current. Any such signal (proportional to the volume of the conversion region) is amplified by the APD and contributes significant shot noise.

Avalanche region: The fabrication techniques and the need to maintain gain uniformity across it limit scope for varying this parameter.

Drift region: The use of low resistivity material in the drift region can dramatically reduce the parasitic capacitance of the APD at the cost of the higher overall operating potential needed to deplete this region. Since the total parasitic capacitance applied to the input of a charge amplifier enters linearly into the white noise generated, this is a very significant factor in the performance of the APD. As will be seen below, the $\approx$20pF capacitance of the EG&G device yields to a proportionately lower noise contribution than the 80pF of the S5345LC. One disadvantage of a wide back region is that this region can contribute to the nuclear diode effect.

1.2 The Gain of an APD

The gain characteristics of an APD are dominated by the fact that in silicon both carrier types can multiply (in what follows we assume that the carriers starting the avalanche are electrons). This leads to regenerative amplification with the gain-versus-applied-voltage curve becoming increasing steep and, at a certain value of reverse bias, the familiar process of diode breakdown. The gain process is characterised by the electron and hole amplification coefficients (the equivalent of the Townsend coefficient in gas amplification) α_e and α_p. These coefficients vary exponentially with the electric field in the avalanche region and with the carrier mean free path. It is the dependence of the mean free path on the ambient temperature which results in the rather strong, negative temperature coefficient of the gain (typically $\approx$-10%/C). The stability of the gain process (and thus the maximum gain permissible before breakdown occurs) is determined by the ratio α_p/α_e (=k). Since α_e and α_p are both rapid functions of the electric field and tend towards each other at high field strengths, the effective value of k (some sort of average over the avalanche region) is strongly dependent on the detailed structure of the avalanche region. Low fields give a low k-value with a high ultimate gain and a stable (i.e. low noise) amplification process. High fields (i.e. narrow junctions) give the reverse. For both the devices under test we observe a maximum gain in the region of 500 and it appears that k is of the order of a few percent.

1.3 Excess Noise

The avalanche process is a statistical process and inevitably noisy. The model developed by MacIntyre [2] defines the excess noise factor as the ratio by which the avalanche process increases the intrinsic shot noise power of the incident light signal. He shows that (approximately)

$$F = kM + (2-1/M)(1-k) \quad (1)$$

which simplifies to $F = 2 + kM$ for $M > 10$. If hole multiplication is absent then $F = 2$ which is the statistical noise contribution due to a simple electron avalanche; however, the onset of hole multiplication (which grows rapidly as the gain is increased) adds the term kM. With $k=0.035$ this term doubles F at a gain of ≈ 60.

The noise of the EG&G diode seems to fit this model well; but that of the S5345LC does not. We can only conclude that the differences in device structure are responsible.

1.4 White Noise Contributions

As noted above, the capacitance and series resistance of the APD contribute to the amplifier noise term which can be expressed in terms of electrons:

$$\sigma_a = 1/q\{2kTRC^2 1.85/\tau\}^{1/2}$$

where q is the electronic charge, R is the total series noise resistance of APD and the amplifier and C is all the parasitic capacity of both APD, wiring and amplifier input device. τ is the amplifier RC shaping time constant and k Boltzmann's constant. The usual FET amplifier input device can have a parallel capacitance of a few pF and a mutual conductance of 30mS (i.e. a noise resistance of $\approx 30\Omega$). Thus, in general the APD capacitance will dominate in determining the amplifier noise term and the contact resistance of the APD will not be significant unless it approaches 30Ω.

Shot noise caused by the APD leakage current has two components: a surface leakage term and a bulk leakage term. The surface leakage results from current flowing around the edge of the APD and is essentially ohmic. Since most of the gain occurs over a small range bias voltage, it can be treated as approximately constant and combined with the amplifier term. The bulk leakage current arises from thermal carrier generation within the active region of the APD and suffers from the disadvantage that it constitutes a signal for the avalanche region and is amplified accordingly. This makes it a serious contribution to the total device noise. In terms of electrons we have a noise contribution from the shot noise:

$$\sigma_{sh} = \{1/q\ (I_s + I_b M^2 F)\ 1.85\tau\}^{1/2}$$

where q is the electronic charge, I_s and I_b the surface and bulk leakage currents, M the APD gain and F the excess noise factor.

1.5 A Noise Model

If we inject N photoelectrons into the APD by means of a light flash the variance on the amplified signal will now be:

$$\sigma^2 = M^2FN + \sigma_{sh}^2 + \sigma_a^2 \quad (2)$$

If we redefine σ_a to include the surface leakage shot noise term we can write:

$$\sigma^2 = M^2FN + M^2F\sigma_b^2 + \sigma_a^2$$

where σ_b is the RMS electron contribution from thermal generation in the APD. The two right-hand terms represent the white noise measured in the system by injecting a charge signal at the amplifier input and the first term represents the poisson statistics which can be observed by illuminating the APD with pulses from a light emitting diode (LED). In the case of an ECAL event we add the signals from nine APD channels so adding the white noise power. Thus:

$$\sigma^2 = M^2FN + 9M^2F\sigma_b^2 + 9\sigma_a^2 \qquad (2a)$$

Having evaluated the gain curve M(V), the excess noise factor F(M) and the two noise contributions σ_a and σ_b from measurements on the two devices it is possible to predict the performance of the ECAL and compare these predictions with the data taken in 1994.

2. MEASUREMENTS

2.1 The Experimental Setup

The APD under test was set up in a light-tight enclosure, connected with very short leads to one channel of the electronic system developed at RAL for the 1994 beam test. This consisted of two small surface-mount printed circuit boards, the first holding the charge amplifier and the second various services such as bias supply monitoring and temperature monitoring. Figure 2 shows the preamplifier design. RC shaping time constants of 27ns are used and the overall gain is 2.4 μV/electron into 50Ω. A test signal may be injected into the amplifier input by means of a 1pF capacitor.

A stable light test pulse was provided by a SiC blue-emitting diode (Hewlett Packard type HLMP-DB00) driven by a cabled-shaped 45V pulse, 20ns wide, from a mercury-wetted relay pulser. The emission wavelength of the diode (481nm peak) is well-suited to the simulation of light from lead tungstate; the only undesirable feature is a significant tail in the time distribution of the emission which stretches to $\approx$200ns.

The APD pulses are fed from the amplifier via a fast (5ns risetime) linear amplifier to an EG&G LG102A integrating linear gate which, in turn feeds an Ortec pulse height analyser (PHA). The linear gate integrates over the pulse width ($\approx$200ns) and so yields lower noise figures than will be encountered using peak sampling (by around 2/3).

All measurements were made at an ambient temperature of around 21C.

2.2 Gain and Noise Measurements

The mean amplitude and noise width of any pulse height distribution generated in the PHA by a light signal incident on the APD is readily calibrated in terms of charge at the amplifier input by the use of the 1pF test capacitor. However, assessment of the noise width in terms of the input photoelectron signal (which is the point of determination of the quality of the

light signal) depends on a knowledge of the APD gain which turns out to rather difficult to measure accurately. It was hoped that a plateau region of pulse height would be observed at low applied bias, which could be identified with the device operating at unity gain. Unfortunately this does not happen with either diode. A second approach is to measure the output pulse height when the APD is irradiated with an xray line which deposits a known amount of charge in the conversion region of the APD (278 electrons/keV of xray energy). The S5345LC gives a reasonable (if rather wide) peak for 5.9keV xrays and a linear response to various xray energies. However, the gain measured in this way is always lower than the value expected from the specification and the gain vs bias curve is very flat compared to that measured with light pulses. This leads one to suspect saturation effects which vitiates this approach as a simple way of calibrating the APD gain. Finally, there is the method proposed by Webb [3] in which a noise measurement is used to evaluate the noise and gain of the APD simultaneously.

2.3 The Webb Method

If we return to the noise formula (2) above and combine the shot noise term with the amplifier noise term (the combination is automatically measured as the white noise σ_w seen as the width of the peak given by the charge test pulser in the PHA) we have:

$$\sigma^2 = M^2FN + \sigma_w^2$$

Substituting the approximation $F = 2 + kM$ and also $M = x/N$ where x is the observed pulse height and N is the number of photoelectrons initiating the avalanche in the APD, we have:

$$(\sigma^2 - \sigma_w^2)/x^2 = 2/N + xk/N^2 \qquad (3)$$

Thus if one plots the left hand side of this relation against the pulse height as the bias voltage is varied, one expects to see a linear relationship. The intercept on the y axis gives the number of initial photoelectrons and the slope gives (in combination with N) the α_p/α_e ratio (k) which in turn determines the excess noise factor (F).

2.4 Measurements using the Webb Method

The EG&G APD (serial no.8) was exposed to the LED and the pulse height distributions recorded as the bias was increased from 300V to 375V in six steps producing a range of peak pulse heights (x) from 10^5 to $5x10^5$ electrons. The standard deviations of both the LED curves (σ) and the charge pulser curves (σ_w) were calculated and the parameter $(\sigma^2 - \sigma_w^2)/x^2$ plotted as a function of x. Figure 3 shows that a reasonable straight line results and fitting indicates that we have N=9569 electrons and k = 0.032. The value of N permits us to calculate the gain function (figure 4) and the value of k specifies the excess noise factor (via equation (1) above). It is interesting to note that the values of k measured by Webb for devices of the same specification (0.034-0.036) are in reasonable agreement with our data.

Applying the same technique to the S5345LC produces less satisfactory results as figure 5

shows; clearly, a straight line is not in evidence. Turning to the data sheet for the S5345 we see that according to the data presented the excess noise factor of this device does not follow the MacIntyre model. In fact we see that:

$$F = aM^b$$

where a and b are functions of wavelength and at 650nm a=0.764 and b=0.349. Rewriting relation (3) with this expression for F we obtain:

$$(\sigma^2 - \sigma_w^2)/x^2 = ax^b/N^{(b+1)}$$

Over most of the data this provides a reasonable fit (figure 5). The fit values are N=7999 electrons, a=0.573 and b=0.291. These are rather better than the values quoted for a wavelength of 650nm and seem plausible for our wavelength of 481nm.

With these measurements in hand we can now compare the excess noise factors of the two devices. Figure 6 shows F as a function of gain. Clearly the S5345LC has a very considerable advantage over the EG&G device at high gains, though it is difficult to understand the mechanism by which the device preserves a value of F less than the "minimum" of 2 up to gains of the order 100.

2.5 Gain Fits

Even the most approximate theoretical model for the gain (vs bias) of an APD is very complex and unsuitable for rapid fitting. We have found a parameterisation which works very well over the gain range of interest to us (M>10). This is:

$$M = (1 + e^{(a+bV)})(1 + e^{(c+dV)})$$

where a,b,c and d are constants. The smooth line through the experimental values of M (obtained from the Webb method) in figure 4 is such a fit.

2.6 White Noise Measurements.

The white noise in the system (consisting of the sum of the diode shot noise and the amplifier noise) is measured as the width of the charge calibration pulse peaks as observed on the PHA. As figure 4 shows, the white noise of the EG&G APD shows virtually no increase with gain up to a gain of $\approx$100. Fitting the noise to the model $\sigma_s = \sqrt{(\sigma_a^2 + M^2\sigma_b^2)}$ in which we approximate by assuming the surface leakage is constant and we incorporate the excess noise factor into σ_b leads to values of σ_a=1722 electrons and σ_b=8.4 electrons. Dividing the measured noise by the gain yields the white noise referred to the input which is a useful parameter. According to our measurements this parameter minimises at $\approx$43 electrons RMS at a gain of $\approx$150.

The results of the same analysis performed on the S5345LC diode are shown in figure 7. The basic amplifier noise is 3026 electrons (reflecting the higher capacitance of this device) and the bulk shot noise term σ_b rises to a value of 103 electrons. This effect is manifest in a

dramatic rise of the white noise as the APD gain is increased. In this device the optimum white noise referred to the input is 100 electrons and occurs at a gain of about 200.

2.7 Gain Measurement using Xrays

The Webb method of gain calibration appears to give a good result with the EG&G device, though the applicability of it to the S5345LC is more debatable. It is, however, a fairly tedious process, unsuited to dealing with large numbers of devices. We have therefore studied the interaction of xrays with the APDs in some detail to see if the undoubted presence of an accurately known charge deposit in the conversion region can be exploited for calibration purposes. It is immediately apparent that the shape of the pulse height versus bias curve is very different for xrays from that for light pulses; in particular the gain for xrays appears to saturate at about 10% of the maximum gain of a light pulse. This is attributed to the dense cloud of initial electrons causing self-shielding from the amplifying field in the avalanche region. Figure 8 shows the gain curves observed in the S5345LC with 5.9keV and 22keV xrays. The slope of the 22keV xray curve is flatter than that of the 5.9keV curve indicating that the saturation depends on the total charge in the cloud. The large energy deposit of the 22keV signal does, however, allow us to observe the peak down to low gains (x4) where the saturation effects may be expected to abate. In figure 8 the LED pulse height curve has been normalised to the 22keV xray curve at low gains (where it is seen to conform well) and the gain of the xray curve in this region is assumed to be linear. Thus the light gain curve can be calibrated. Figure 9 shows the light gain curve derived in this manner plotted with the gain curve derived from the calibration of the Webb method. The agreement is within about 20% which appears reasonable given the quality of the fit in figure 5. The clean and stable response of these diodes to xrays encourages us to believe that the method of setting up the gains on the xray peaks (as we did for the 1994 test run) is viable.

The response of the EG&G diode to xrays is (in contrast with the S5345LC) very complex. With 5.9keV xrays, when the gain approaches 10, two peaks are observed. The upper two curves in figure 10 show the calculated gain for these peaks. The upper is assumed to correspond to detection of the xrays in the conversion region but the location of the conversion of the second peak is a mystery (conversion in the avalanche region would not be expected to give rise to an identifiable peak). When the device is irradiated with high energy xrays (42keV) a clear response is obtained at the highest applied bias with an observed gain of less than four at maximum. This is interpreted as the multiplication of the hole cloud drifting back from xray conversions in the 100μm thick drift region. The gain curve for these signals is also shown in figure 10. The sensitivity to the thick drift region has implications for the nuclear diode effect in the EG&G diode. For example at a bias of $\approx$350V (electron gain $\approx$50) a minimum ionising particle traversing the drift section and experiencing a gain of 2 will generate $\approx$20000 electrons compared a signal of $\approx$30000 from the conversion layer, thus contributing significantly to the nuclear diode effect.

3. MODELLING THE CONTRIBUTION OF THE APD NOISE TO THE ECAL PERFORMANCE.

With the performance parameters in hand we can now model the expected contribution of the

APDs to the performance of the ECAL. It is clear that the EG&G device has the advantages over the S5345LC of low capacity (20pF vs 80pF) leading to proportionately lower amplifier noise and low bulk leakage noise permitting the use of higher gains without amplifying the white noise, but the disadvantage of a higher excess noise factor. Thus the EG&G diode produces better results at low signal levels but at very high signal levels the lower excess noise factor of the S5345LC gives it the advantage.

The parameter calculated in the model is σ/MN i.e. "σ/E" and is derived from relation (2a) above using the experimentally derived parameters for the two diodes. Figure 11 shows estimated performance of the ECAL using the S5345LC diodes in the setup of the 1994 tests. When a constant term of 0.5% is added in quadrature reasonable agreement between the model and the data points is observed. (In all the model plots the abscissa is given in terms of photoelectrons; this enables the plots to be used with any light yield which may be thought appropriate. In the 1994 tests the photoelectron yield was found to be 0.9/MeV; thus our abscissa is approximately in MeV.)

At RAL we are trying to design the best preamplifier for any given APD. (This chiefly involves selecting the FET to suit the APD capacitance.) In figures 12 and 13 the noise parameters have been inserted for the optimum preamplifier configurations for both the EG&G diode and the S5345 (300pF) devices to illustrate the level of performance to be expected in the 1995 beam tests. Apparently, we are promised S5345 diodes with reduced bulk leakage relative to that experienced in the LC devices. If this is the case there will be more gain of resolution with M than is apparent in figure 13. Figure 14 shows a comparison of all the cases studied. It is clear that below $\approx$20GeV the EG&G device is superior while above this the S5345 is superior. It will be noted that in either case one must be above 100GeV before the APD contribution reaches 0.5%. In the case of two APDs viewing the same crystal two identical noise powers are added and one must simply divide the ordinate of the curve by $\sqrt{2}$. (The abscissa remains the number of photoelectrons per APD.)

The remaining factor to be taken into account for the ECAL performance is the effect of radiation damage on the noise of the APDs. In simple terms, radiation damage generates shallow trapping centres which contribute to the thermally-generated bulk leakage current which (as noted above) is amplified by the APD. The fast neutron fluence is expected to be the worst offender in the generation of radiation damage and a visitor to RAL from EG&G indicated that increases of the order $200nA/(10^{12}/cm^2)$ in the leakage current were to be expected, annealing to around half that value after a few weeks. The single crystal material of the EG&G device could be expected to be more sensitive to radiation damage than the epitaxial material of the S5345 so that the advantage experienced by the EG&G APD in the respect of bulk leakage current could soon be eroded by the neutron fluences anticipated. ($10^{12}/cm^2$/year?). At RAL we are commissioning facilities to permit neutron irradiations using our ISIS machine and hope to have results in a few months time.

REFERENCES

[1] G P Heath et al, Status report on a proposal to build subsystem prototypes for the CMS electromagnetic calorimeter, February 1995.

[2] R J McIntyre, IEEE Trans Elec Dev ED-13 (No.1) 1966, 164.

[3] P P Webb, An intrinsic method for the gain and "k factor" characterisation of silicon avalanche photodiodes, EG&G Optoelectronics Canada, VEO-TR-94-012.

FIGURES

1. A schematic section of the structure of an avalanche photodiode.

2. Circuit diagram of the charge-sensitive amplifier used in the tests.

3. A "Webb" plot with the EG&G APD permitting the evaluation of the number of incident photoelectrons and the "k" factor.

4. The white noise and gain of the EG&G APD as evaluated by the Webb method.

5. A Webb plot for the Hamamatsu S5345LC APD.

6. A comparison of the excess noise factor of the EG&G APD and the S5345LC (as evaluated by the Webb method).

7. The white noise and gain of the S5345LC as evaluated by the Webb method.

8. The gain of the S5345LC as measured by 55Fe (5.9keV) and Ag K (22keV) xrays. The pulse height curve of the LED is normalised to the Ag xray data below a bias of 200V.

9. A comparison of the gain curves measured for the S5345LC by the Webb method and the xray method.

10. The gain curves obtained with the various xray peaks observed in the EG&G APD.

11. A comparison of the prediction of the noise model (as applied to the hardware of the 1994 beam test) with the observed data. A constant term of 0.5% is included. The ordinate is "σ/E".

12. The noise performance (σ/E) predicted for the EG&G APDs in the 1995 beam tests with the optimal preamplifier design.

13. The noise performance (σ/E) predicted for the S5345 in the 1995 tests with the optimal preamplifier design.

14. A comparison of the noise performance of all the APD/amplifier options considered.

Figure 1

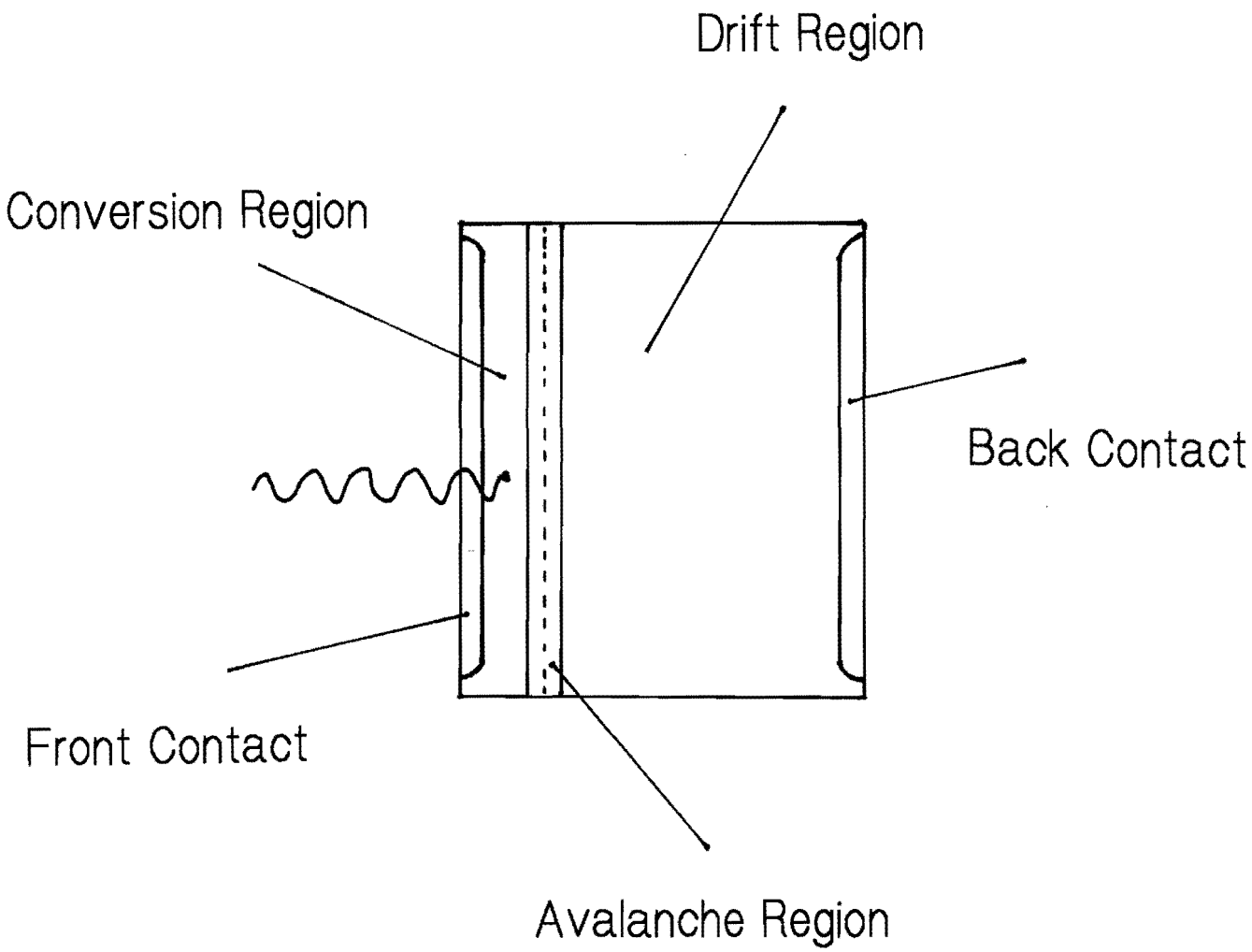
Drift Region
Conversion Region
Back Contact
Front Contact
Avalanche Region

Figure 2

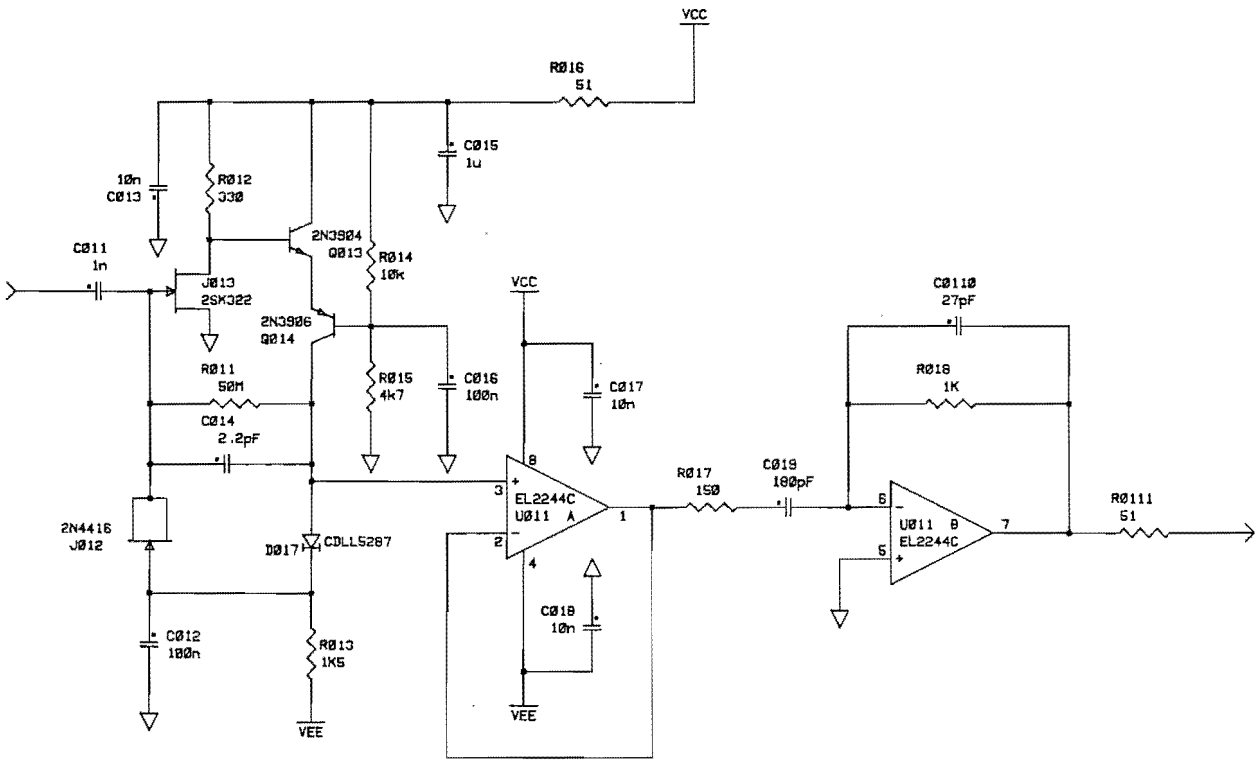
VCC
R016
51
C015
1u
10n
C013
R012
330
2N3904
Q013
R014
10k
C011
1n
J013
2SK322
2N3906
Q014
VCC
C0110
27pF
R011
50M
R015
4k7
C016
100n
C017
10n
R018
1K
C014
2.2pF
8
3
EL2244C
U011 A
1
2
4
R017
150
C019
100pF
6
U011 B
EL2244C
7
5
R0111
51
2N4416
J012
D017
CDLL5287
C018
10n
C012
100n
R013
1K5
VEE
VEE

Figure 3

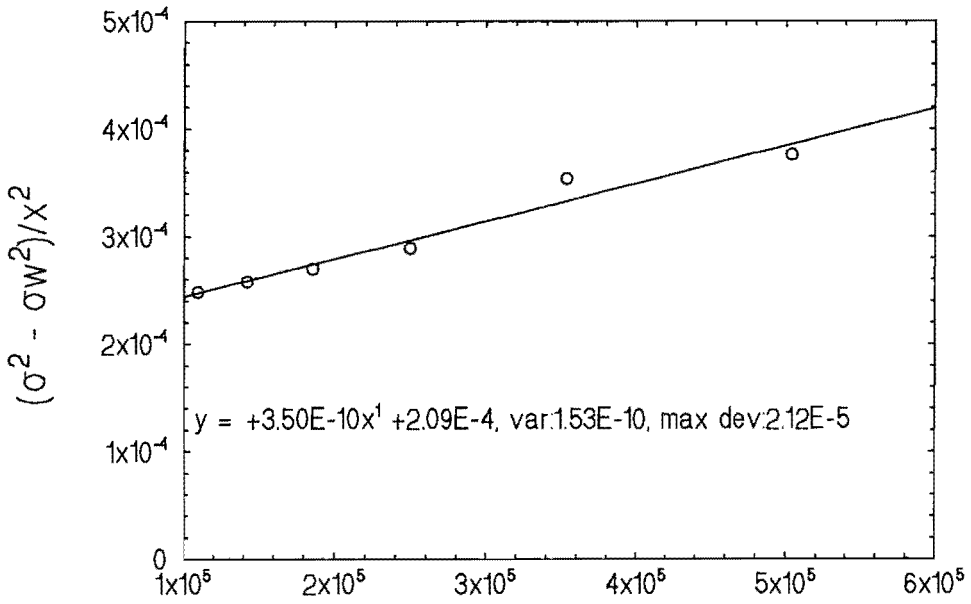

Figure 4

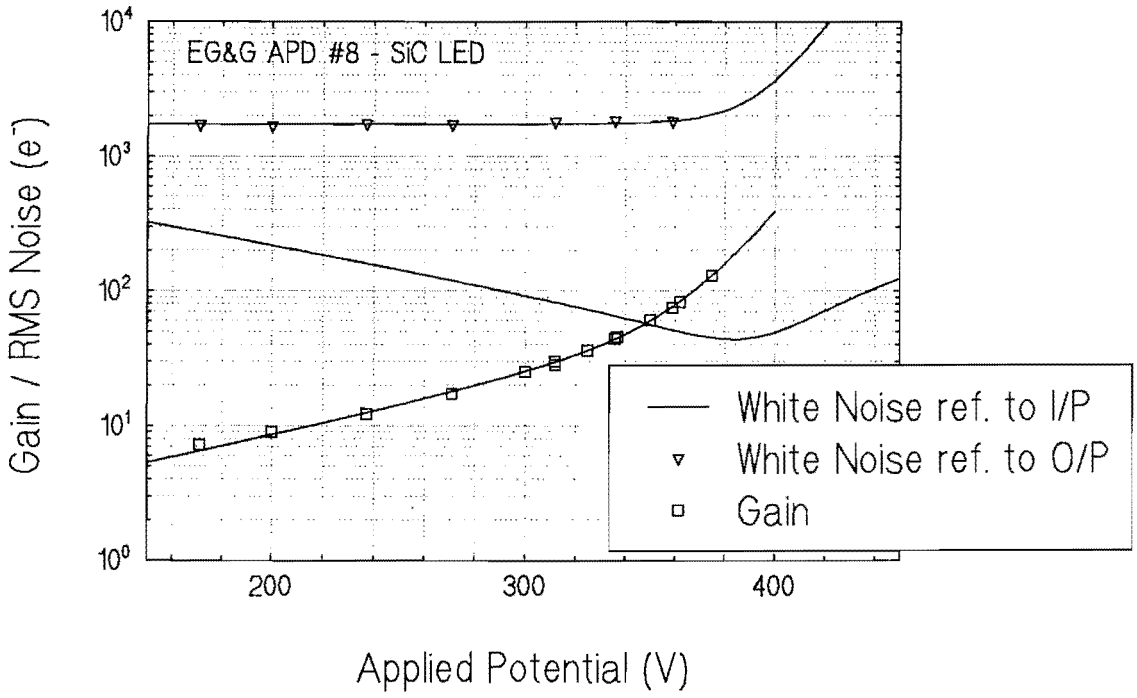

Figure 5

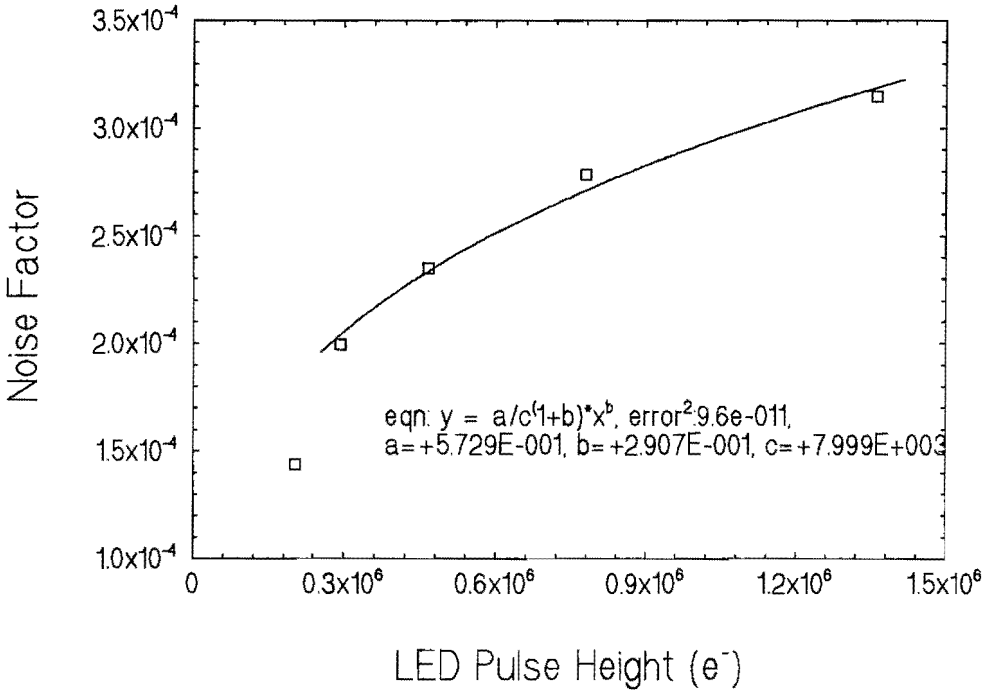

Figure 6

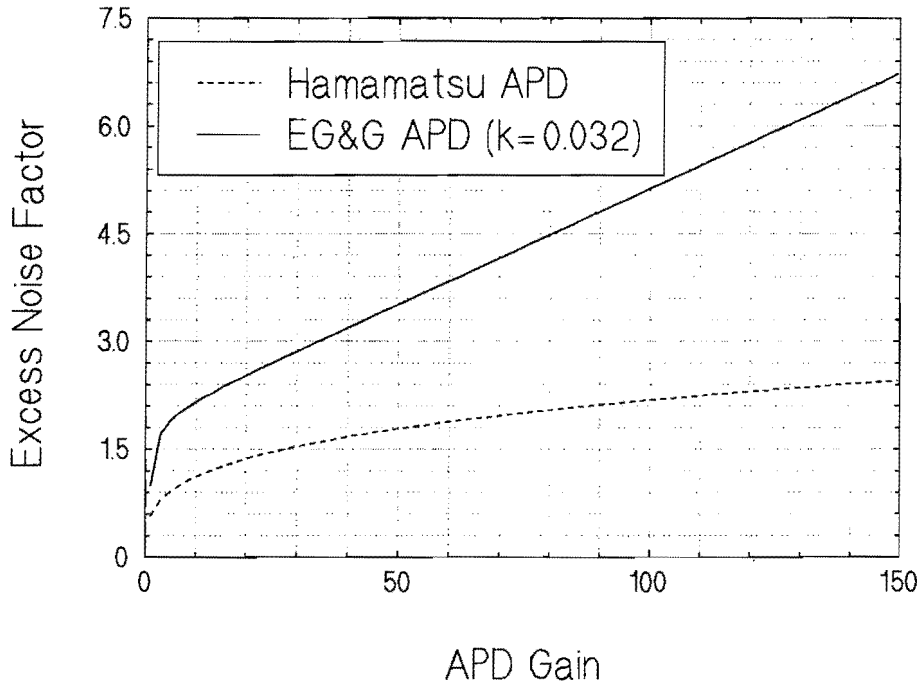

Figure 7

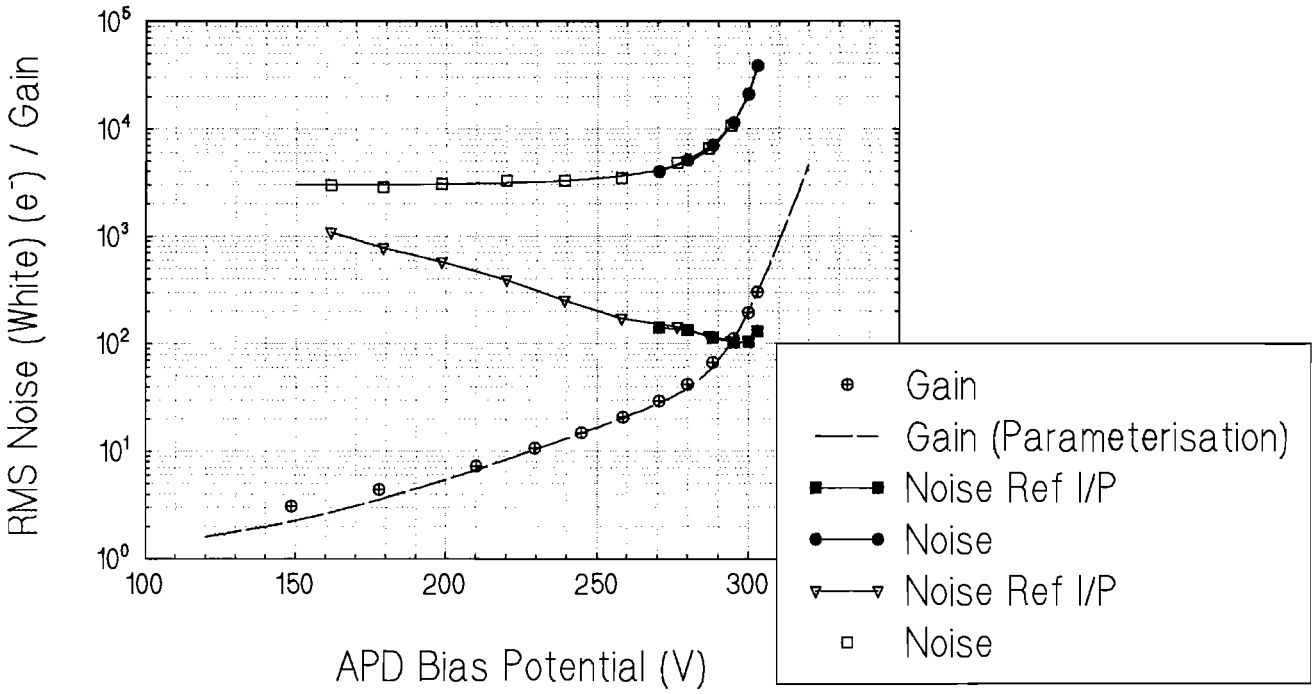

Figure 8

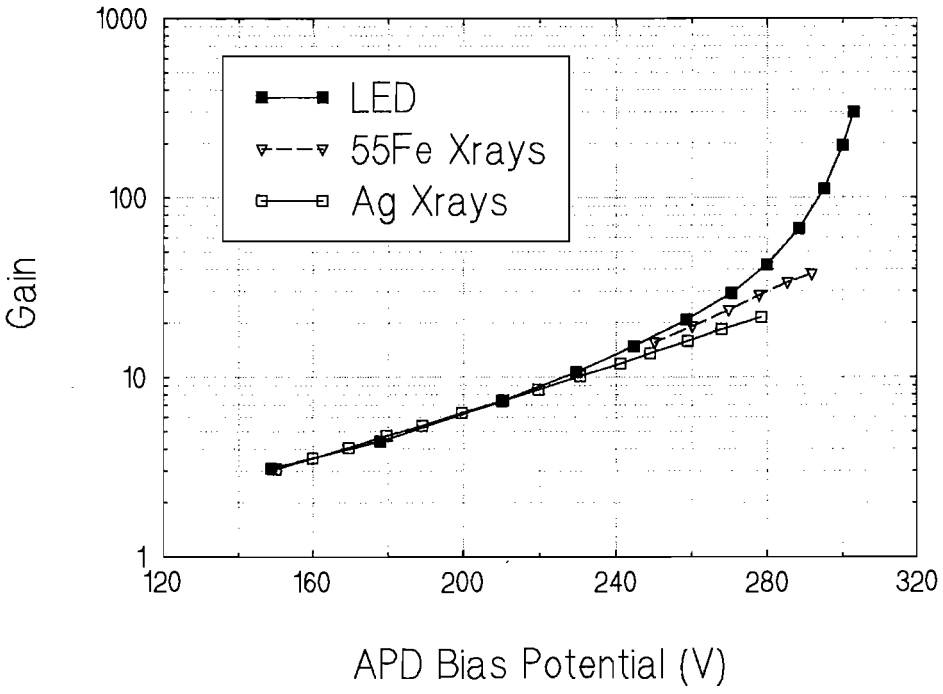

Figure 9

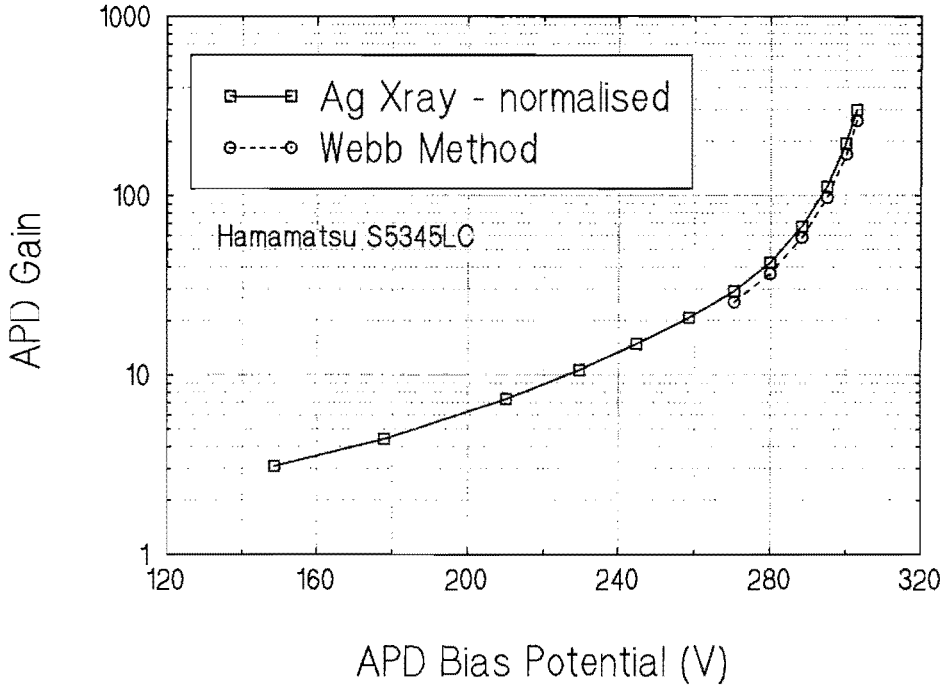

Figure 10

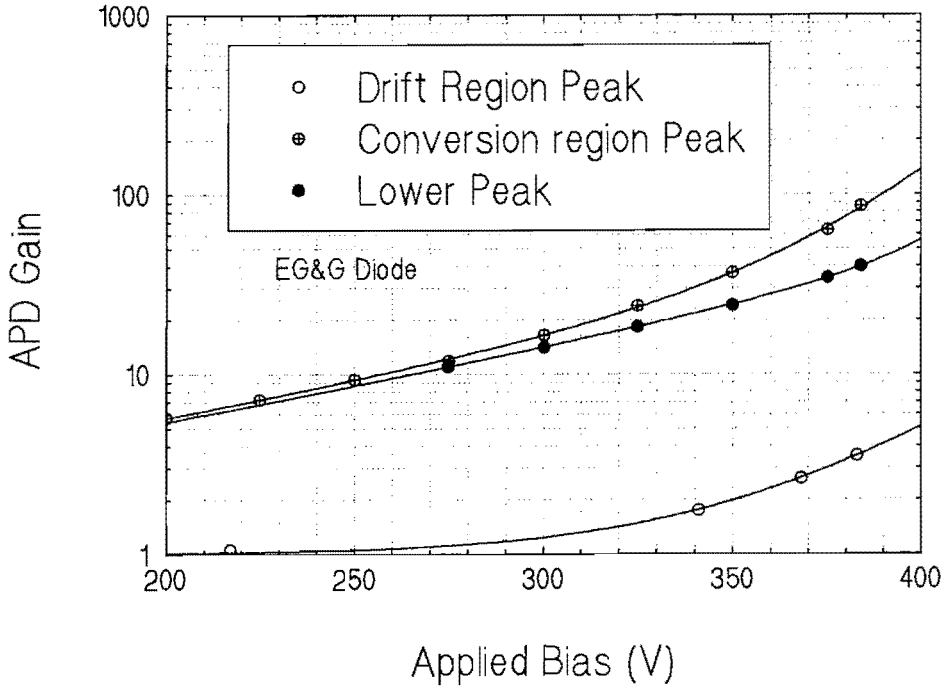

Figure 11

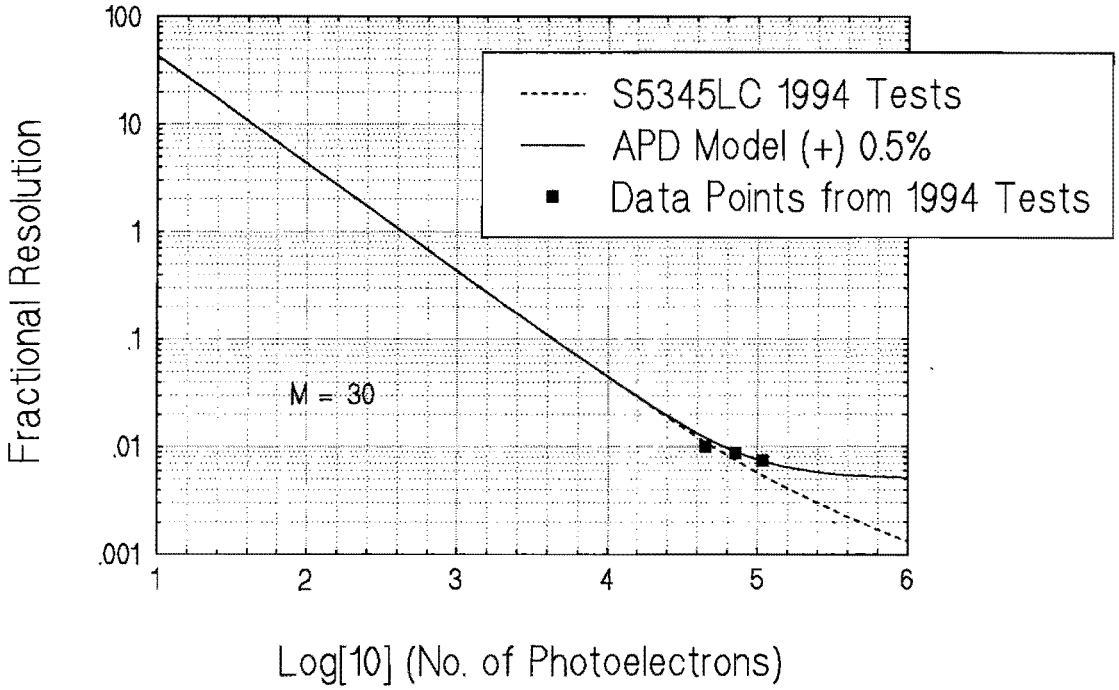

Figure 12

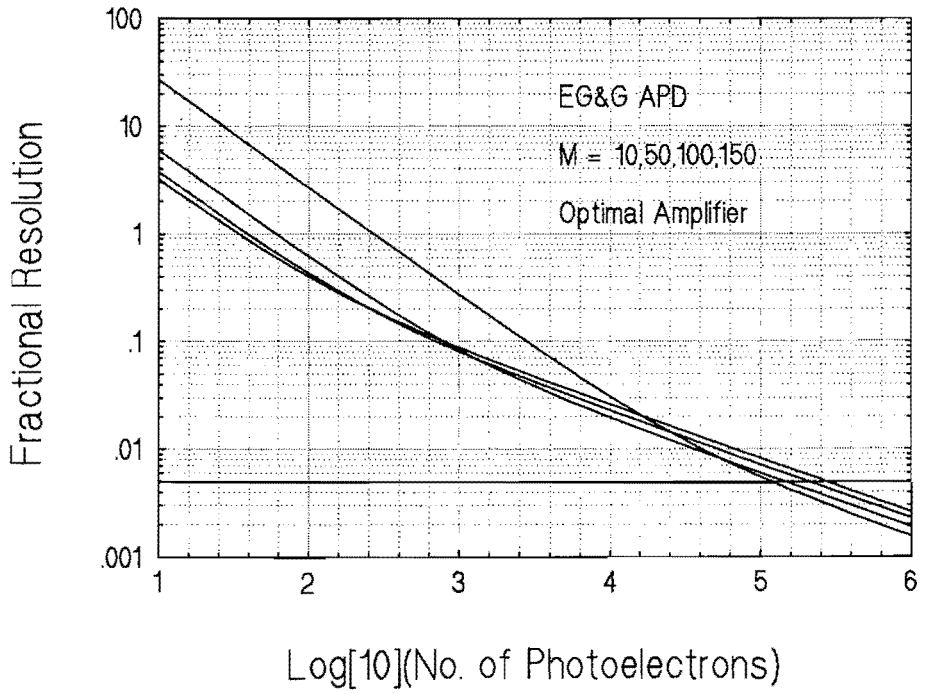

Figure 13

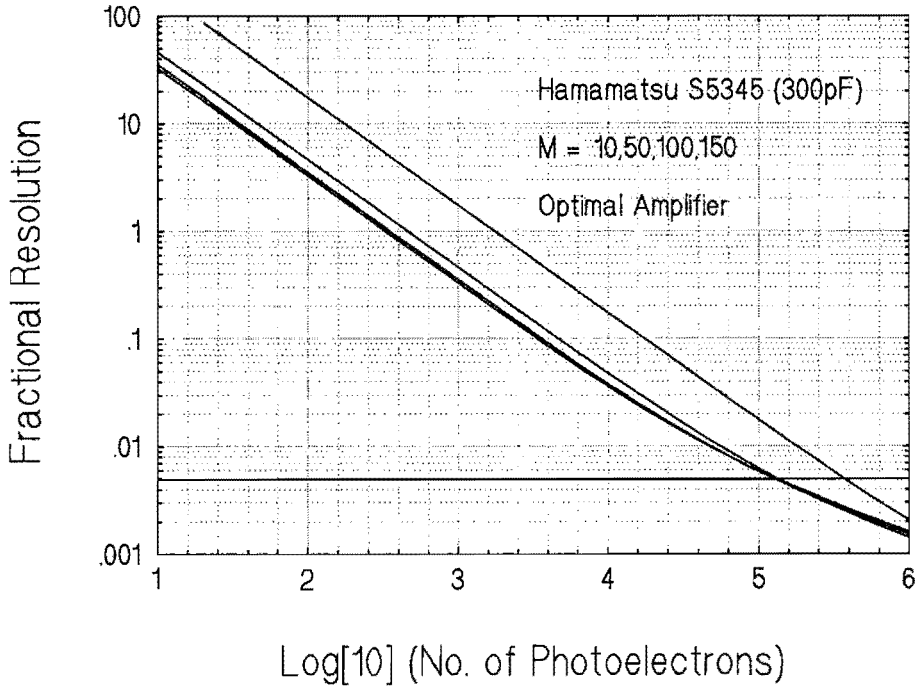

Figure 14